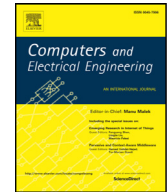




Contents lists available at ScienceDirect

Computers and Electrical Engineering

journal homepage: www.elsevier.com/locate/compeleceng

A novel Gaussian matched filter based on entropy minimization for automatic segmentation of coronary angiograms[☆]

Ivan Cruz-Aceves^{a,*}, Fernando Cervantes-Sanchez^b, Arturo Hernandez-Aguirre^b,
Ricardo Perez-Rodriguez^b, Alberto Ochoa-Zezzatti^c

^a CONACYT Research Fellow - Centro de Investigación en Matemáticas (CIMAT), A.C., Jalisco S/N, Col. Valenciana, C.P. 36000, Guanajuato, Gto, México

^b Centro de Investigación en Matemáticas (CIMAT), A.C., Jalisco S/N, Col. Valenciana, C.P. 36000, Guanajuato, Gto, México

^c Juarez City University, Av. Heroico Colegio Militar S/N, Col. Chamizal, C.P. 88700, Ciudad Juarez, Chihuahua, México

ARTICLE INFO

Article history:

Received 15 October 2015

Revised 3 May 2016

Accepted 3 May 2016

Available online xxx

Keywords:

Automatic segmentation

Coronary arteries

Entropy

Gaussian matched filters

Univariate marginal distribution algorithm

Vessel detection

ABSTRACT

This paper presents a new method for automatic detection and segmentation of coronary arteries in X-ray angiograms. In the vessel detection stage, a novel Gaussian matched filter (GMF) based on an entropy minimization fitness function is used to detect blood vessels in angiographic images. The detection results of the proposed Gaussian matched filter are compared with those obtained by five state-of-the-art GMF-based methods using the area (A_z) under the receiver operating characteristic (ROC) curve. In the second stage, the inter-class variance thresholding method has proven to be the most efficient compared with six different methods in order to classify vessel and non vessel pixels from the Gaussian filter response using the accuracy measure and the ground-truth angiograms drawn by a specialist. Finally, the proposed method is compared with eight state-of-the-art vessel segmentation methods. Due to the high rating of similarity (0.97) between the highest A_z value and the A_z value acquired by the fitness function over the whole dataset of angiograms, the result of vessel detection using the proposed GMF demonstrated high performance achieving $A_z = 0.945$ with a test set of 45 angiograms. In addition, the results of vessel segmentation with the inter-class variance thresholding method provided an accuracy of 0.961 with the test set of angiograms.

© 2016 Elsevier Ltd. All rights reserved.

1. Introduction

Automatic segmentation of medical images is a challenging and complex task that has become essential for computer-aided diagnosis (CAD). In recent years, several computational methods have been proposed for the segmentation of human organs and blood vessels from different types of clinical studies such as liver in computed tomography [1], brain and brain tumors in magnetic resonance images [2–4], and blood vessels in retinal fundus images [5] and coronary angiographic

[☆] Reviews processed and recommended for publication to the Editor-in-Chief by Associate Editor Dr. M. R. Daliri.

* Corresponding author. Tel.: +52 473 732 7155/ 735 0800; Ext. 4506; fax: +52 473 732 5749.

E-mail addresses: ivan.cruz@ciimat.mx (I. Cruz-Aceves), fernando.cervantes@ciimat.mx (F. Cervantes-Sanchez), artha@ciimat.mx (A. Hernandez-Aguirre), ricardo.perez@ciimat.mx (R. Perez-Rodriguez), alberto.ochoa@uacj.mx (A. Ochoa-Zezzatti).

<http://dx.doi.org/10.1016/j.compeleceng.2016.05.002>

0045-7906/© 2016 Elsevier Ltd. All rights reserved.

images [6]. The coronary angiography is a specialized X-ray procedure used in cardiology for diagnosing, treating and monitoring coronary artery abnormalities. The main challenges in the segmentation of blood vessels from X-ray coronary angiograms are the non-uniform illumination along vessel structures and the weak contrast between coronary arteries and the image background. Consequently, the coronary artery segmentation problem has been addressed in two different steps; vessel detection also known as vessel enhancement, and classification of vessel-like structures. The first step is used for removing noise from the angiogram while emphasizing vessel-like structures, and in the second step, a classification strategy to discriminate vessel and non vessel pixels is applied.

In the literature, a number of computational methods have been proposed for the automatic detection of vessels in different clinical studies. Some of the state-of-the-art methods are based on mathematical morphology such as the single-scale top-hat operator proposed by Eiho and Qian [7], which was later improved by Qian et al. [8] by introducing a multi-scale top-hat operator based on a linear combination of multiple scales to detect vessels of different diameters. These morphology-based methods present low performance when vessels have weak contrast and different diameters to be detected.

To overcome the disadvantages of the morphology-based techniques, diverse methods using the properties of the Hessian matrix (second-order derivatives) have been proposed [9,10]. These Hessian-based methods perform well in detecting vessel of different diameters as compared to the morphology-based methods; however, due to the use of the second-order derivative of the Gaussian kernel, these methods are highly sensitive to noise. The method of Frangi et al. [9] uses the eigenvalues of the Hessian matrix to compute a measure of vesselness, which is capable of classifying vessel-like structures from the dominant eigenvalues at different scales. From the Hessian matrix, a number of vesselness measures have been proposed in different types of clinical studies [11–13].

Another type of spatial vessel detection techniques based on matching templates has been commonly used. The most frequently applied is the Gaussian matched filters (GMF) proposed by Chaudhuri et al. [14]. The GMF works on the assumption that the blood vessels can be approximated by a Gaussian curve as matching template. This template is rotated at different angular resolutions, and then it is convolved with the given image to form a directional filter bank, and finally the maximum response at each pixel is recorded to acquire the enhanced image. Chanwimaluang and Fan [15,16] used GMF as a detection method for retinal vessel segmentation and registration. Kang et al. [17] proposed a fusion strategy for the segmentation of coronary angiograms consisting of two procedures. The use of the morphology-based top-hat operator and also the GMF method. Both methods are independently applied on the given angiogram, and then, entropy maximizing threshold method is applied on both images. The segmentation result is acquired by pixel-wise multiplication of these two images. The enhancement procedure was also applied in Kang et al. [6,18] using the degree segmentation technique instead of the entropy thresholding method. Cinsdikici and Aydin [19] proposed blood vessel detection method for ophthalmoscope images using the GMF method with a high number of directional filters.

In the GMF-based methods described above, the values for each parameter were experimentally or empirically determined, consequently, the optimal performance of the GMF may not be acquired, since the four parameters of the GMF method have to be tuned for each image specifically to obtain the highest detection performance. Al-Rawi et al. [20] proposed an improved GMF method for retinal images by introducing a search space for each variable, and an exhaustive global search strategy was applied to find the optimal values by using a training set of images. Cruz et al. [21] proposed a new range of values for GMF to be applied on coronary angiograms, and an estimation of distribution algorithm was applied to obtain the optimal parameters using a training set and the area under the receiver operating characteristic (ROC) curve as fitness function. The main disadvantages of these training-based methods, is that the fitness function is an exhaustive thresholding technique that requires the hand-labeled angiograms performed by a specialist, and also that the distribution of the hand-labeled angiograms in the training and testing sets could be different.

In the present paper, a new method for automatic detection and segmentation of coronary arteries in X-ray angiograms is proposed. In the detection stage, a novel Gaussian matched filter based on an entropy minimization function is introduced to automatically enhance vessel-like structures, while avoiding training-based methods requiring an exhaustive global search and ground-truth images, or empirically determined values. To assess the performance of the proposed fitness function with respect to the area under the ROC curve, the relative error is employed. Moreover, to evaluate the performance of the proposed GMF method with respect to different detection methods of the state-of-the-art, the area under the ROC curve is used. In the second stage, in order to classify vessel and non vessel pixels from the Gaussian filter response, seven thresholding methods are compared to obtain the highest vessel segmentation in terms of accuracy. Finally, the segmentation results of the proposed method are compared and evaluated with those obtained with eight, previously mentioned, state-of-the-art vessel segmentation methods.

2. Methods

2.1. Gaussian matched filters

The Gaussian matched filters (GMF) were proposed by Chaudhuri et al. [14] for detecting blood vessels in low contrast retinal images. The fundamental idea of the GMF is that the gray-level profile of the cross section of a vessel-like structure can be approximated in the spatial image domain by using a Gaussian shaped curve as matching template. The Gaussian

template is defined as follows:

$$G(x, y) = -\exp\left(-\frac{x^2 + y^2}{2\sigma^2}\right), \quad |y| \leq L/2, \quad (1)$$

where L is a discrete parameter (in pixels) that represents the length of the vessel segment to be detected, and the σ parameter is used to approximate the average width of blood vessels. Due to the Gaussian curve has infinitely long double sided trails, these trails are commonly truncated at $u = \pm 3\sigma$, where a discrete parameter T is used to define a neighborhood N , and also to determine the position in the matching template where the Gaussian curve trails will cut as follows:

$$N = \{(u, v), |u| \leq T, |v| \leq L/2\}. \quad (2)$$

On the other hand, to detect vessel-like structures at different orientations, the Gaussian kernel $G(x, y)$ can be rotated to different angular resolutions (θ) by applying a geometric transformation to form a bank of $\kappa = 180^\circ/\theta$, evenly spaced filters as follows:

$$\kappa = \begin{bmatrix} \cos \theta_i & -\sin \theta_i \\ \sin \theta_i & \cos \theta_i \end{bmatrix}, \quad (3)$$

where $\theta_i = (i\pi/\kappa)$, $i = \{1, 2, \dots, \kappa\}$ is the orientation of the filters, and κ is the number of oriented filters in the range $[-\frac{\pi}{2}, \frac{\pi}{2}]$. These oriented filters are convolved with the original image, and for each pixel, the maximum response over all orientations is conserved to generate the final enhanced image.

Since the GMF is controlled by the continuous parameter σ , and the discrete parameters L , T , and κ , the selection of the optimal values for the GMF parameters plays an essential role for each particular application in order to obtain the highest vessel detection performance. In Fig. 1, an X-ray angiogram is enhanced by using two Gaussian templates with different sets of values with the aim of providing a visual comparative analysis of the resulting filtered images (Fig. 1(f) and (i)). The first Gaussian template (Fig. 1(c), (d) and (e)) corresponds to the fixed values $L = 9$, $T = 13$, and $\sigma = 2.0$ as it was firstly proposed by Chaudhuri et al. [14], and the second Gaussian template (Fig. 1(g) and (h)) corresponds to the fixed values $L = 7$, $T = 15$, and $\sigma = 2.0$.

In general, the GMF parameters have been experimentally or empirically determined, as well as by using the area (A_2) under the ROC curve, however, to compute the ROC curve, the hand-labeled images of the original angiograms are required.

2.2. Estimation of distribution algorithms

Estimation of distribution algorithms (EDAs) are stochastic optimization methods that incorporate statistical information of candidate solutions to solve numerical problems in discrete and continuous domain [22]. Similar to evolutionary computation techniques, EDAs use a population of candidate solutions also known as individuals, selection operators, and binary or real encoding to perform the optimization task. The main idea of EDAs resides in the fact that the new potential solutions are created by building a probabilistic model based on global statistical information of promising individuals, instead of applying the crossover and mutation operators. In the present work, the Univariate Marginal Distribution Algorithm (UMDA) with binary encoding has been adopted because of the nature of the GMF optimization problem, since UMDA works ideally for problems with not many significant dependencies [23].

UMDA generates a probability vector $\mathbf{p} = (p_1, p_2, \dots, p_n)^T$ to build the probabilistic model in order to create new individuals for each variable independently, where p_i is a marginal probability rate. This probability vector is used to approximate the probability distribution of the current individuals in \mathbb{P}_t as the product of the univariate frequencies computed from a subset of potential solutions assuming that all the variables are independent. The process carried out by UMDA can be summarized in the three steps of selection of promising solutions, estimation of probability distribution, and production of new individuals. In the selection step, the individuals in the search space Ω are arranged according to the fitness value, then a probability s is calculated through proportional selection as follows:

$$\mathbb{P}^s(x) = \frac{\mathbb{P}(x)f(x)}{\sum_{\tilde{x} \in \Omega} \mathbb{P}(\tilde{x})f(\tilde{x})}. \quad (4)$$

In the second step, the estimation of the univariate marginal probabilities \mathbb{P} are computed, where the probability model for independent variables can be defined as follows:

$$\mathbb{P}(x) = \prod_{i=1}^n \mathbb{P}(X_i = x_i), \quad (5)$$

where $x = (x_1, x_2, \dots, x_n)^T$ represents the binary value of the i th bit in the individual, and X_i is the i th random value (obtained from a uniform distribution) of the vector X . The third step is used to generate new individuals by using the estimated probability distribution, which is evaluated by the fitness function at each generation, and finally, these three steps are iteratively performed until a convergence criterion is satisfied.

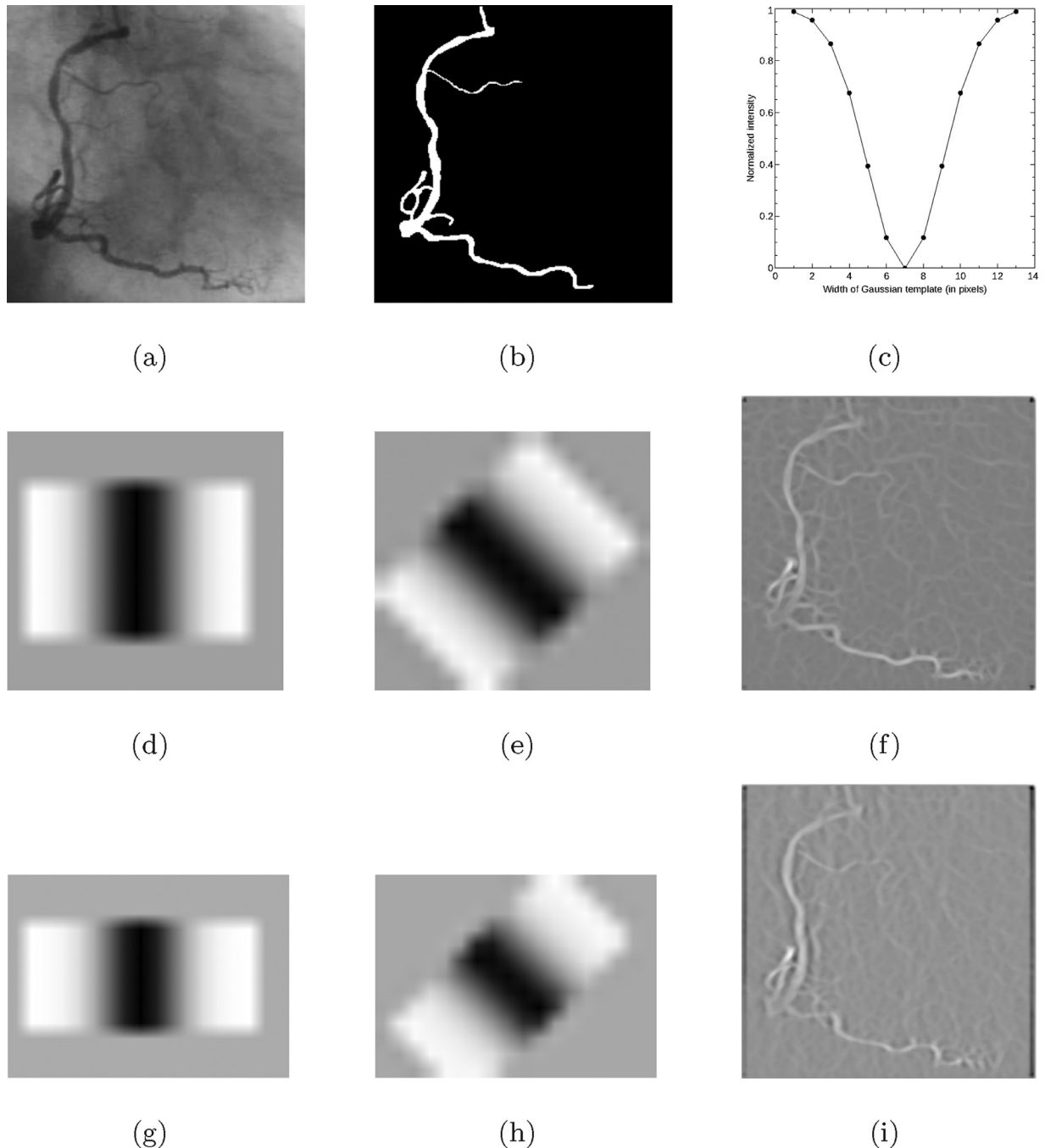


Fig. 1. (a) Original X-ray coronary angiogram. (b) Ground-truth of angiogram in (a). (c) Gaussian profile proposed by Chaudhuri et al. [14]. (d) and (e) Gaussian template applying $\sigma = 2.0$, $L = 9$, $T = 13$, and $\theta = 0^\circ$, and $\theta = 45^\circ$, respectively. (f) Enhanced image using the angiogram in (a) and the templates in (d) and (e). (g) and (h) Gaussian template assigning $\sigma = 2.0$, $L = 7$, $T = 15$, and $\theta = 0^\circ$, and $\theta = 45^\circ$, respectively. (i) Enhanced image using the angiogram in (a) and the templates in (g) and (h).

2.3. Optimization of the Gaussian matched filters

Due to the detection performance of the GMF method directly depends of four parameters, many researchers have proposed different values for each parameter of the filter. According to the original work of Chaudhuri et al. [14], these parameters were experimentally determined as $L = 9$, $T = 13$, $\sigma = 2.0$, and $\theta = 15$, obtaining $\kappa = 12$ oriented filters. Cinsdikici and Aydin [19], applied the original values of L , T , and σ , modifying the angular resolution to $\theta = 10^\circ$ obtaining $\kappa = 18$ oriented

filters. Kang et al. [6,17,18] modified the value of the average vessel width to $\sigma = 1.5$, and the angular resolution of $\theta = 30$ degrees obtaining 6 oriented filters.

On the other hand, to avoid empirically or experimentally determined values for each parameter, some methodologies have been proposed. Al-Rawi et al. [20] modified the GMF method by introducing a range of values for each parameter as $L = \{7, 7.1, \dots, 11\}$, $T = \{2, 2.25, \dots, 10\}$, and $\sigma = \{1.5, 1.6, \dots, 3\}$, keeping constant the number of oriented filters to $\kappa = 12$. In this method, an exhaustive global search is applied over all possible combinations of the extended variables, and the area A_z under the receiver operating characteristic (ROC) curve is used to select the best set of values for the GMF method. Cruz et al. [21] proposed to extend the range of the variables to $L = \{8, 9, \dots, 15\}$, $T = \{8, 9, \dots, 15\}$, $\sigma = \{1, 6\}$ with step size of 0.001, and $\kappa = 12$ oriented filters. The best set of GMF parameters was determined by using the A_z values of a training set, and applying an Estimation of distribution algorithm to avoid the exhaustive global search.

In general, the GMF method has been used with empirically or experimentally determined values, or by using the values acquired from a training procedure through the A_z values. The detection results acquired from the training procedure presents superior performance than the empirically defined methods in terms of blood vessel detection; however, the performance can be improved since the distribution of the training set can be different from the test set, due to the hand-labeled angiograms performed by experts. In the present work, a new strategy based on a novel entropy minimization objective function, which is minimized by applying UMDA is proposed. The search space of the GMF parameters was defined according to the features of the X-ray coronary angiograms, and the state-of-the-art GMF methods described above. The search space of the variables was defined as $L = \{3, 5, 7, \dots, 17\}$, $T = \{3, 5, 7, \dots, 17\}$, $\kappa = \{10, 12, 15, 18, 30, 45, 60, 90\}$, and $\sigma = \{1, 6\}$ with step size of 0.1. The binary encoding of UMDA is set to 18 bits, where 9 bits are used for the parameter σ , and the remaining three parameters (L, T, κ) are set to 3 bits each one.

2.3.1. Fitness function

Generally, a suitable detection performance of the GMF method involves a high number of connected edges. In the proposed function, the entropy of the Gaussian matched filter response and the edge pixels are used as fitness value for each individual of UMDA. This fitness function, which has to be minimized, is presented below:

$$fitness(x) = entropy(I_{gmf} \cdot I_{gmf_{edge}}). \quad (6)$$

From the fitness function, $fitness(x)$ denotes the fitness value of individual x , I_{gmf} represents the Gaussian matched filter response of the given angiogram I , and $I_{gmf_{edge}}$ denotes the edge image of the enhanced angiogram applying the Sobel edge detector, which can be defined as follows:

$$\begin{aligned} \delta h(i, j) &= g_1(x+1, y-1) + 2g_1(x+1, y) + g_1(x+1, y+1) \\ &= -g_1(x-1, y-1) - 2g_1(x-1, y) - g_1(x-1, y+1) \end{aligned} \quad (7)$$

$$\begin{aligned} \delta v(i, j) &= g_1(x-1, y+1) + 2g_1(x, y+1) + g_1(x+1, y+1) \\ &= -g_1(x-1, y-1) - 2g_1(x, y-1) - g_1(x+1, y-1) \end{aligned} \quad (8)$$

where $\delta h(i, j)$ and $\delta v(i, j)$ represent the horizontal and vertical gradient operations of the edge detector, which are convolved with I_{gmf} , in order to obtain $I_{gmf_{edge}}$.

The GMF methods based on the A_z values, require the hand-labeled angiograms (ground-truth) outlined by experts in order to perform their training stage, which pose different disadvantages when working with medical images. Since the proposed fitness function only uses information from the enhanced angiogram, a training stage to select the most appropriate values for the GMF parameter is not required.

2.4. Inter-class variance thresholding method

The inter-class variance thresholding method proposed by Otsu [24], assumes that the input image has a bi-modal histogram containing two classes of pixels. This method is applied on the histogram of intensity levels, and it can be described by using the following three steps.

Firstly, the mean intensity of the given image has to be determined, which can be calculated by using the following:

$$\mu = \sum_{i=1}^L i P_i, \quad (9)$$

where L is the number of intensity levels $\{0, 1, 2, \dots, L-1\}$, and P_i represents the probability distribution computed through the number of pixels n_i with intensity i , and using the total number of pixels N as follows:

$$P_i = \frac{n_i}{N}. \quad (10)$$

Secondly, the mean intensity for each independent class of pixels has to be determined, which can be computed by using the following:

$$\mu_j = \sum_{i=t_{j-1}+1}^{t_j} \frac{iP_i}{w_j} \quad (11)$$

where w_j represents the probability distribution for each class of pixels having a threshold intensity value t . Finally, the inter-class variance is computed as follows:

$$\sigma^2 = \sum_{j=1}^n w_j (\mu_j - \mu)^2, \quad (12)$$

where the optimal threshold value corresponds to the intensity value with the maximum inter-class variance. This last step, can be defined as the maximization of the inter-class variance criterion as follows:

$$\phi = \max_{1 < t_1 < \dots < t_{n-1} < L} \{\sigma^2(t)\}. \quad (13)$$

2.5. Evaluation measures

In order to assess the performance of the blood vessel detection and segmentation methods in the present work, the area under the receiver operating characteristic (ROC) curve, as well as the accuracy measure have been adopted.

The ROC curve uses the true-positive fraction (TPF) and the false-positive fraction (FPF) of a classification system. The ROC curve is computed by using a sliding threshold to a gray-scale filter-response image, where the different results are compared with the corresponding ground-truth angiogram to obtain a plot of TPF and FPF values. In order to approximate the area (A_z) under the ROC curve, the Riemann-sum method is applied. In the present work, the A_z value is used to evaluate the performance of the vessel detection methods using the test set of angiograms, as well as to select their most appropriate parameters using the training set.

To evaluate the performance of the vessel segmentation results, the accuracy measure is used. The accuracy measure has been widely used as the main measure for evaluation of binary classification problems, which is defined as the fraction of correctly classified pixels divided by the number of pixels in the image as follows:

$$\text{Accuracy} = \frac{TP + TN}{TP + FP + TN + FN}, \quad (14)$$

where TP and TN are the fractions of vessel and non vessel pixels correctly classified as such by the method, respectively. FP represents the fraction of non vessel pixels that are incorrectly classified, and FN is the fraction of vessel pixels incorrectly classified by the method.

3. Results and discussion

In this section, the database of X-ray coronary angiograms used in the present work is introduced. Furthermore, since the proposed coronary artery segmentation method is divided into two stages, the proposed vessel detection method, and the results of vessel segmentation are presented and discussed in different sections. The computational experiments were implemented in the Matlab software version 2014a, on a computer with an AMD-A10, 8GB of RAM, and 3.7 GHz processor.

3.1. Coronary angiograms

The database used in the present work consists of 90 X-ray coronary angiograms of 29 patients. Each angiogram is of size 300×300 pixels, and the vessel ground-truth for each image was outlined by a specialist. The ethics approval was provided by the cardiology department of the Mexican Social Security Institute, UMAE T1 León. In the experiments, 45 of the 90 angiograms are used as training set for tuning the parameters of the different comparative methods, and the remaining 45 angiograms are used as test set for evaluation of the vessel detection and segmentation methods.

3.2. Evaluation of vessel detection

The proposed fitness function Eq. (6) for coronary artery detection using the GMF method, has been compared with the performance obtained from the area A_z through the test set of angiograms. In Fig. 2(a), the highest A_z value is compared with the A_z value acquired by the fitness function for each angiogram in the test set. In Fig. 2(b), the relative error between the highest A_z value obtained by the ROC curve analysis and the A_z value acquired by the minimization of the fitness function is illustrated. In terms of correctness with the highest A_z value, the proposed fitness function obtains 0.97 over the whole database of X-ray coronary angiograms, which is an advantage taking into account that the fitness function only requires the Gaussian filter response, and a training procedure involving the hand-labeled angiograms is avoided.

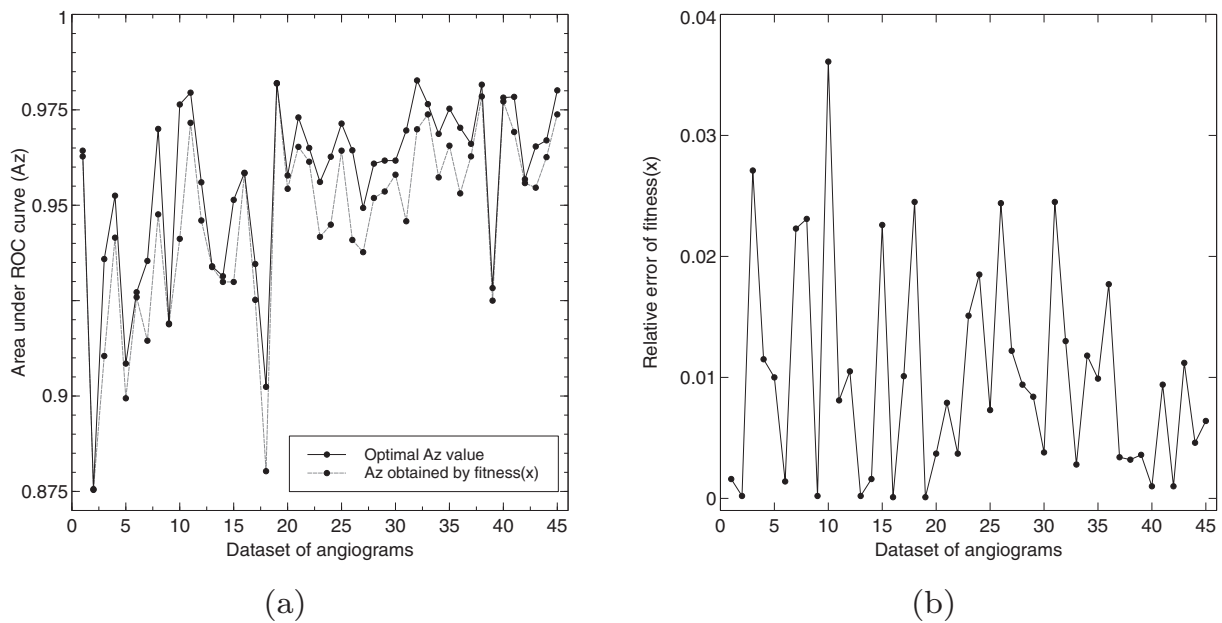


Fig. 2. (a) Comparative analysis of the proposed fitness function with the highest area A_z using the test set of angiograms. (b) Relative error of the fitness function for each angiogram in the test set, in terms of area A_z .

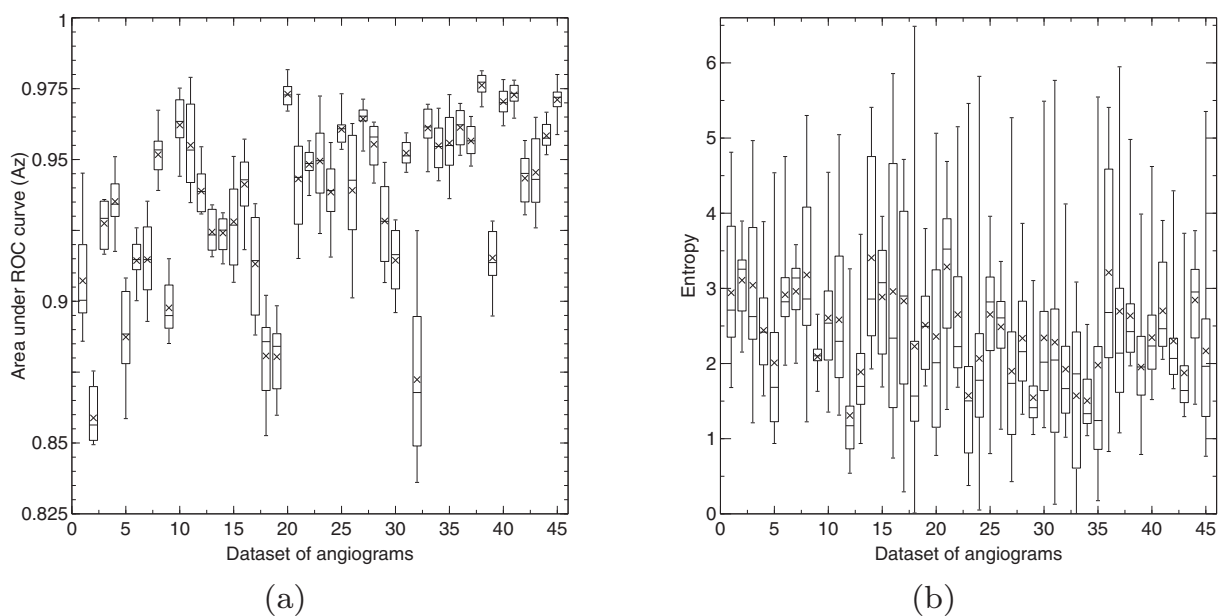


Fig. 3. Distribution of the solutions obtained with 30 trials of UMDA over the test set of angiograms. (a) Maximizing the area A_z , and (b) minimizing the $fitness(x)$.

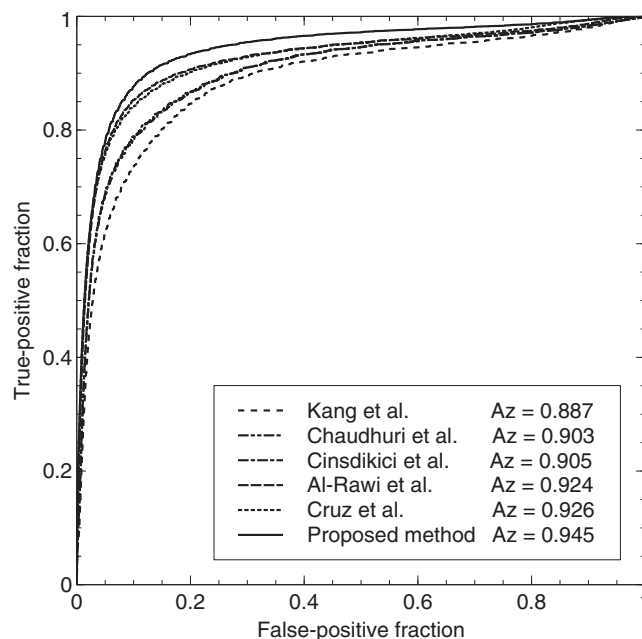
In order to minimize the proposed fitness function, UMDA was applied with a population size = 30 and selection rate = 0.6. The distribution of 30 trials for each angiogram in the test set, is presented in Fig. 3. The optimization process is applied to minimize the fitness function through the entropy measure involved in it, which directly increases the A_z at the same time, although the ROC curve analysis can be omitted, since it is not required. The distribution of both results is shown in Fig. 3(a) and Fig. 3(b), respectively.

As part of the comparative analysis between the proposed GMF based on entropy minimization method and different GMF methods of the state-of-the-art, in Table 1 the best set of parameters for each comparative method is shown. From Table 1, the methods of Chaudhuri et al. [14], Cinsdikici and Aydin [19], and Kang et al. [17] show values reported

Table 1

Optimal parameters of different GMF vessel detection methods of the state-of-the-art.

Vessel detection method	Parameters					
Chaudhuri et al. [14–16]	$\sigma = 2.0$	$L = 9$	$T = 13$	$\kappa = 12$	$\theta = 15^\circ$	$S = 19$
Cinsdikici and Aydin [19]	$\sigma = 2.0$	$L = 9$	$T = 13$	$\kappa = 18$	$\theta = 10^\circ$	
Kang et al. [6,17,18]	$\sigma = 1.5$	$L = 9$	$T = 13$	$\kappa = 6$	$\theta = 30^\circ$	
Al-Rawi et al. [20]	$\sigma = 1.9$	$L = 11$	$T = 9$	$\kappa = 12$	$\theta = 15^\circ$	
Cruz et al. [21]	$\sigma = 2.41$	$L = 15$	$T = 15$	$\kappa = 12$	$\theta = 15^\circ$	

**Fig. 4.** Comparison of ROC curves for vessel detection with the test set of 45 angiograms using the GMF response obtained from the proposed and comparative methods.

experimentally or empirically determined. On the other hand, the methods of Al-Rawi et al. [20] and Cruz et al. [21] present values obtained through a training procedure with the reported range of variables, using the training set.

Using the best set of parameters described above, Fig. 4 illustrates the ROC curves and area A_z obtained by applying the different GMF methods on the test set of angiograms. The comparative analysis reveals that the proposed GMF method provide a higher performance in vessel detection than the comparative five methods. The method proposed by Kang et al [6,17,18], obtains the lowest vessel detection, due to the method uses empirically determined values for the GMF parameters of σ and number of evenly spaced filters κ . The methods of Chaudhuri et al. [14], and Cinsdikici and Aydin [19] present similar vessel detection performance, since the main difference between both methods, is the GMF parameter of number of oriented filters κ , with different angular resolution θ . The methods of Al-Rawi et al. [20], and Cruz et al. [21] obtain superior performance than the experimentally determined methods because in these two strategies, the search space of the GMF parameters was modified and the best set of values to be applied on a test set, was determined using a training set of angiograms. The performance in terms of area A_z of the proposed method, shows that the fitness function is suitable for the detection of coronary arteries in X-ray angiograms, which introduces two main advantages with the state-of-the-art methods described above; firstly, the high level of differentiation between vessel and background pixels regarding the comparative methods; and secondly, the novel methodology to compute appropriate parameters for the GMF method, which avoids training procedures with hand-labeled angiograms and also empirically determined values. Additionally, in order to visualize the detection results, Fig. 5 presents a subset of angiograms with the corresponding ground-truth and the vessel detection results of the aforementioned methods.

3.3. Evaluation of vessel segmentation

To classify vessel and non vessel pixels from the Gaussian matched filter response of the proposed method, seven automatic thresholding methods of the state-of-the-art have been compared in terms of accuracy; the results are presented in Table 2. The measure of accuracy is used in the experiments, since it has been widely used in the literature for evaluation

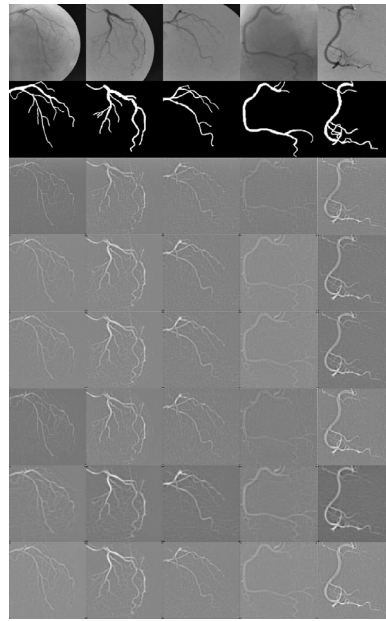


Fig. 5. First row: subset of angiograms from the test set. Second row: ground-truth of images in the first row. The remaining six rows show the GMF response of the methods of Kang et al. [17], Chaudhuri et al. [14], Cinsdikici et al. [19], Al-Rawi et al. [20], Cruz et al. [21], and proposed method, respectively, applied to the angiograms in the first row.

Table 2

Comparative analysis of seven state-of-the-art thresholding methods applied to the Gaussian matched filter response of the proposed method using the test set of 45 angiograms.

Thresholding method	Accuracy
Kapur et al. [25]	0.354
Rosenfeld and De La Torre [26]	0.570
Tsai [27]	0.580
Pal and Pal [28]	0.824
RATS [29]	0.929
Ridler and Calvard [30]	0.958
Otsu [24]	0.961

Table 3

Comparative analysis of the proposed method with respect to eight state-of-the-art vessel segmentation methods using the test set of 45 angiographic images.

Segmentation method	Accuracy
Chanwimaluang and Fan [15]	0.860
Kang et al. [17]	0.901
Al-Rawi et al. [20]	0.932
Tsai et al. [13]	0.933
Li et al. [11]	0.950
Qian et al. [8]	0.951
Wang et al. [12]	0.953
Kang et al. [6]	0.954
Proposed method	0.961

and comparison of vessel segmentation methods. These results show that the inter-class variance method [24] provides the highest segmentation performance when compared with the other six thresholding methods. The segmentation results represent the average of the test set. Due to its performance in both measures, the inter-class variance thresholding method is chosen for further analysis.

In Table 3, the proposed coronary artery segmentation method consisting of the application of Gaussian matched filters with an entropy minimization function for vessel detection followed by the inter-class variance thresholding method for classification is compared with eight state-of-the-art vessel segmentation methods using a test set of 45 angiograms. In

Table 4

Average execution times (per angiogram) for the proposed method as compared with the state-of-the-art vessel segmentation methods.

Segmentation method	Execution time (seconds)	Training time (seconds)
Chanwimaluang and Fan [15]	2.28	–
Kang et al. [17]	2.24	64.72
Al-Rawi et al. [20]	2.03	1610.55
Tsai et al. [13]	1.87	1175.43
Li et al. [11]	1.95	60.29
Qian et al. [8]	1.46	1023.47
Wang et al. [12]	1.79	61.43
Kang et al. [6]	2.81	64.72
Proposed method	6.38	–

this comparative analysis, the method of Chanwimaluang and Fan [15], uses the original parameters of the GMF proposed by Chaudhuri et al. [14]. The methods of Kang et al. [6,17] in addition to using the GMF with the parameter discussed above (see Table 1), the classical morphology-based top-hat operator is also applied. The top-hat operator is governed by two main parameters; shape of the structuring element, and its size. The optimal parameters for the top-hat operator were determined via the area A_z under the ROC curve using the training set of angiograms as disk-shaped structuring element with size = 19 pixels. The method of Al-Rawi et al. [20] was performed by applying the parameters described above for vessel detection, and the threshold value was chosen according to the best trade-off of TPF and FPF of the ROC curve as 0.65. Since the methods of Li et al. [11], and Wang et al. [12] use the properties of the eigenvalues computed from the Hessian matrix, they were tuned with scales in the range [1, 20] with step sizes in the range $\delta = [0.5, 4.0]$. The method of Tsai et al. [13] in addition to using the parameters of scale and step size for the Hessian matrix, the parameters of weighting factor w , constant of normalization c , threshold value T , and intensity factor *factor* have to be tuned. These parameters were determined by using the training set of angiograms via the A_z value. The method of Qian et al. [8] is governed by the number of disk-shaped structuring elements and their corresponding size S_n . The optimal parameters of the method were determined by varying the size of the structuring elements in the range [3, 21] with the training set of angiograms. The comparative analysis shows that the proposed method provides the highest performance in terms of accuracy in relation to the state-of-the-art vessel segmentation methods using the test set of angiograms. In addition, this analysis has also shown that the methods based on an optimization process or with a training procedure obtain a higher performance than the empirically determined methods in terms of segmentation accuracy.

Table 4 presents the execution time of the comparative vessel segmentation methods. Since the proposed method computes the optimal parameters for each particular image by minimizing a fitness function, a training time is not required. This optimization process increases the computational time regarding the execution of the comparative methods, although in terms of global time (execution and training time), the proposed method achieves competitive results. The computational complexity of the proposed enhancement method can be calculated by decomposing the fitness function, where the number of operations to compute the GMF is given by the size of the Gaussian template (LT) to be rotated κ times in order to be convolved with input image, which can be expressed as $\mathcal{O}(M^2)$. The convolution to compute the Sobel operator (mask of size 3×3) on the Gaussian filter response is also $\mathcal{O}(M^2)$. The product between the Gaussian filter response and the resulting Sobel edge response can be expressed as matrix multiplication operation given $\mathcal{O}(M^3)$, and finally, the computation of the entropy measure can be defined as $\mathcal{O}(M^2)$.

Fig. 6 presents a subset of coronary angiograms from the test set with the corresponding vessel ground-truth for each angiogram. The method of Chanwimaluang and Fan [15] obtains the lowest performance due to the high rate of background pixels incorrectly classified as vessel pixels. The results of the method of Kang et al. [17] show low detection rate in angiograms with weak contrast between vessels and background image, obtaining low performance in terms of vessel pixels correctly classified as such by the method. The method of Al-Rawi et al. [20] presents a high rate of broken vessels and also a low rate of true-positives pixels, which decrease the performance of the accuracy measure. The results of the method of Tsai et al. [13] shows adequate rate of true-positive pixels; however, the high rate of background pixels incorrectly classified as vessel pixels affects its performance. The method of Li et al. [11] detects vessels of different calibers; however, the low rate of correctly classified vessel pixels decreases its performance. The main drawback of the method of Qian et al. [8], is the detection of vessels of different diameters, which decreases the performance in terms of accuracy. The method of Wang et al. [12] shows uniform segmentation along the vessel-like structures at different calibers while presenting many broken vessels. These drawbacks of the method decrease the performance of the accuracy measure, since a low rate of vessel pixels are detected. The results of the method of Kang et al. [6], which performs the degree segmentation method instead of the entropy criterion ([17]), presents low performance in angiograms having non-uniform illumination and with vessels having low contrast, which affects the accuracy performance. The results obtained from the proposed method present the highest segmentation performance in terms of accuracy obtaining a low rate of broken vessels and false-positives pixels.

The vessel segmentation methods of the state-of-the-art discussed above provide adequate performance in terms of area A_z under the ROC curve and segmentation accuracy. The comparative analysis reveals that the GMF based on entropy

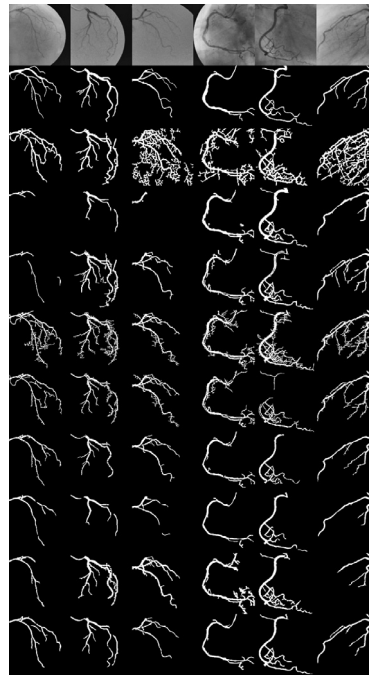


Fig. 6. First row: subset of angiograms from the test set. Second row: ground-truth for the images corresponding to the first row. The remaining nine rows present the segmentation results of the methods of Chanwimaluang and Fan [15], Kang et al. [17], Al-Rawi et al. [20], Tsai et al. [13], Li et al. [11], Qian et al. [8], Wang et al. [12], Kang et al. [6], and our proposed method, respectively, applied to the angiograms in the first row.

minimization is robust for working with angiograms having uneven illumination along vessel-like structures, and the inter-class variance thresholding method is suitable for classification of vessel and non vessel pixels, providing the highest accuracy of blood vessel segmentation.

4. Conclusion

In this paper, a new method for automatic detection and segmentation of coronary arteries in X-ray angiograms has been introduced. In the vessel detection stage, a novel Gaussian matched filter based on an entropy minimization function has demonstrated to be more efficient than five state-of-the-art GMF-based methods, achieving $A_z = 0.945$ with the test set of angiograms. Additionally, the proposed fitness function has also shown that a training procedure requiring the hand-labeled angiograms can be omitted due to the high rating of similarity (0.97) between the highest A_z value and the A_z value acquired by the fitness function. Moreover, in the vessel segmentation stage, the inter-class variance thresholding method has proven to be the most efficient compared with six different methods, obtaining a segmentation accuracy of 0.961 with the test set of 45 X-ray coronary angiograms. According to the experimental results, the proposed method consisting of the application of Gaussian matched filters based on an entropy minimization fitness function for vessel detection followed by the inter-class variance thresholding method for classification of vessel pixels, can lead to higher accuracy than eight vessel segmentation methods.

Acknowledgment

This research has been supported by the National Council of Science and Technology of México (Cátedras-CONACYT No. 3150-3097).

References

- [1] Kumar S, Moni R, Rajeesh J. An automatic computer-aided diagnosis system for liver tumours on computed tomography images. *Comput Electric Eng* 2013;39:1516–26.
- [2] Ahmadvand A, Daliri M. Improving the runtime of MRF based method for MRI brain segmentation. *Appl Math Comput* 2015;256:808–18.
- [3] Nabizadeh N, Kubat M. Brain tumors detection and segmentation in MR images: gabor wavelet vs. statistical features. *Comput Electric Eng* 2015;45:286–301.
- [4] Ahmadvand A, Shariffar M, Daliri M. Supervised segmentation of MRI brain images using combination of multiple classifiers. *Australasian Phys Eng Sci Medicine* 2015;38:241–53.
- [5] Mittal D, Kumari K. Automated detection and segmentation of drusen in retinal fundus images. *Comput Electric Eng* 2015;47:82–95.
- [6] Kang W, Kang W, Li Y, Wang Q. The segmentation method of degree-based fusion algorithm for coronary angiograms. In: *2nd International Conference Measurement, Information and Control*; 2013. p. 696–9.

- [7] Eiho S, Qian Y. Detection of coronary artery tree using morphological operator. *Comput Cardiol* 1997;24:525–8.
- [8] Qian Y, Eiho S, Sugimoto N, Fujita M. Automatic extraction of coronary artery tree on coronary angiograms by morphological operators. *Comput Cardiol* 1998;25:765–8.
- [9] Frangi A, Niessen W, Vincken K, Viergever M. Multiscale vessel enhancement filtering. In: *Medical Image Computing and Computer-Assisted Intervention (MICCAI'98)*, 1496. Springer LNCS; 1998. p. 130–7.
- [10] Shikata H, Hoffman E, Sonka M. Automated segmentation of pulmonary vascular tree from 3D CT images. In: *Proceedings SPIE International Symposium Medical Imaging*, 5369; 2004. p. 107–16.
- [11] Li Y, Zhou S, Wu J, Ma X, Peng K. A novel method of vessel segmentation for X-ray coronary angiography images. In: *Fourth International Conference on Computational and Information Sciences (ICIS)*; 2012. p. 468–71.
- [12] Wang S, Li B, Zhou S. A segmentation method of coronary angiograms based on multi-scale filtering and region-growing. In: *International Conference on Biomedical Engineering and Biotechnology*; 2012. p. 678–81.
- [13] Tsai T, Lee H, Chen M. Adaptive segmentation of vessels from coronary angiograms using multi-scale filtering. In: *International Conference on Signal-Image Technology and Internet-Based Systems*; 2013. p. 143–7.
- [14] Chaudhuri S, Chatterjee S, Katz N, Nelson M, Goldbaum M. Detection of blood vessels in retinal images using two-dimensional matched filters. *IEEE Trans Medical Imaging* 1989;8(3):263–9.
- [15] Chanwimaluang T, Fan G. An efficient blood vessel detection algorithm for retinal images using local entropy thresholding. In: *Proceedings IEEE International Symposium on Circuits and Systems*, 5; 2003. p. 21–4.
- [16] Chanwimaluang T, Fan G, Fransen S. Hybrid retinal image registration. *IEEE Trans Inform Technol Biomedicine* 2006;10(1):129–42.
- [17] Kang W, Wang K, Chen W, Kang W. Segmentation method based on fusion algorithm for coronary angiograms. In: *2nd International Congress on Image and Signal Processing (CISP)*; 2009. p. 1–4.
- [18] Kang W, Kang W, Chen W, Liu B, Wu W. Segmentation method of degree-based transition region extraction for coronary angiograms. In: *2nd International Conference on Advanced Computer Control*; 2010. p. 466–70.
- [19] Cinsdikici M, Aydin D. Detection of blood vessels in ophthalmoscope images using MF/ant (matched filter/ant colony) algorithm. *Comput Methods Programs in Biomedicine* 2009;96:85–95.
- [20] Al-Rawi M, Qutaishat M, Arrar M. An improved matched filter for blood vessel detection of digital retinal images. *Comput Biol Medicine* 2007;37:262–7.
- [21] Cruz-Aceves I, Hernandez-Aguirre A, Valdez-Pena I. Automatic coronary artery segmentation based on matched filters and estimation of distribution algorithms. In: *Proceedings of the 2015 International Conference on Image Processing, Computer Vision, & Pattern Recognition (ICCV'2015)*; 2015. p. 405–10.
- [22] Hauschild M, Pelikan M. An introduction and survey of estimation of distribution algorithms. *Swarm Evolutionary Comput* 2011;1(3):111–28.
- [23] Bashir S, Naeem M, Shah S. A comparative study of heuristic algorithms: GA and UMDA in spatially multiplexed communication systems. *Eng Appl Artificial Intel* 2010;23:95–101.
- [24] Otsu N. A threshold selection method from gray-level histograms. *IEEE Trans Systems, Man Cybernetics* 1979;9(1):62–6.
- [25] Kapur J, Sahoo P, Wong A. A new method for gray-level picture thresholding using the entropy of the histogram. *Comput Vision, Graphics Image Process* 1985;29:273–85.
- [26] Rosenfeld A, De la Torre P. Histogram concavity analysis as an aid in threshold selection. *IEEE Trans Systems, Man Cybernetics* 1983;13:231–5.
- [27] Tsai W. Moment-preserving thresholding: a new approach. *Comput Vision, Graphics, and Image Process* 1985;29:377–93.
- [28] Pal NR, Pal SK. Entropic thresholding. *Signal Process* 1989;16:97–108.
- [29] Kittler J, Illingworth J, Föglein J. Threshold selection based on a simple image statistic. *Comput Vision, Graphics Image Process* 1985;30:125–47.
- [30] Ridler T, Calvard S. Picture thresholding using an iterative selection method. *IEEE Trans Systems, Man Cybernetics* 1978;8:630–2.

Ivan Cruz-Aceves received a Ph.D. in Electrical Engineering from University of Guanajuato in 2014. He works at the Mexican National Council on Science and Technology assigned to the Center for Research in Mathematics since 2014. His research areas are biomedical signal and image analysis, computational intelligence, and evolutionary computation.

Fernando Cervantes-Sanchez received a Bachelor Degree in Statistical Industrial Engineering from the Autonomous University of Aguascalientes, Mexico during 2013. He studies a M.Sc. in Computer Sciences and Industrial Mathematics at the Center for Research in Mathematics. His research areas are medical image processing and evolutionary computation.

Arturo Hernandez-Aguirre received a PhD. in Computer Science from Tulane University in 2001. He is the author of over 30 journal papers and over 100 conference papers. He currently serves as associate editor of Computational Optimization and Computation Journal. His main research interests are: i) evolutionary computation, and ii) estimation of distribution algorithms.

Ricardo Perez-Rodriguez received a PhD in Industrial Engineering. He has published work related on evolutionary computing and simulation applied on service and manufacturing systems on different journals. His main research areas are discrete-event simulation, simulation optimization, and evolutionary computing.

Alberto Ochoa-Zezzatti (Ph.D.'04, Postdoctoral Researcher,'06, and Industrial Postdoctoral Research '09). He joined the Juarez City University in 2008. He has 7 books, and 27 chapters in books related with AI. He has supervised 17 Ph.D. theses, 27 M.Sc. theses and 29 undergraduate theses.